

PACS numbers: 81.07.Wx; 81.05.Je; 42.70.Hj
DOI: 10.1070/QE2013v043n03ABEH015138

Nanopowders M_2O_3 (M = Y, La, Yb, Nd) with spherical particles and laser ceramics based on them

S.N. Bagayev, A.A. Kaminskii, Yu.L. Kopylov, V.B. Kravchenko, A.V. Tolmachev, V.V. Shemet, R.P. Yavetskiy

Abstract. **We have considered the problems of agglomeration of yttrium aluminium garnet (YAG) nanopowders prepared by chemical co-precipitation of precursors from aqueous solutions and subsequent calcination. To fabricate YAG and Y_2O_3 laser ceramic samples with high optical transmittance and reproducible characteristics, we have developed a method for producing non-agglomerated nanopowders of pure and doped Y_2O_3 by homogeneous chemical precipitation. Nanopowders Y_2O_3 with La and Yb as well as mixtures of Y_2O_3:Nd and several commercial nanopowders of aluminium oxide have been compacted; optimised compacting technique have been selected; ceramic samples $(Y, La, Yb)_2O_3$ and YAG:Nd with high optical transmittance at a wavelength of 1 μm have been produced by solid-phase synthesis.**

Keywords: *laser ceramics, nanopowders, yttrium aluminium garnet, yttrium oxide, spherical nanoparticles, optical transmission.*

1. Introduction

In recent years significant progress has been made in the development of laser oxide ceramics and in increasing (to values above 100 kW) output powers in quasi-cw regime of solid-state lasers using active elements of oxide ceramics, mainly on the basis of yttrium aluminium garnet (YAG), yttrium oxides and rare earth elements. This topic has been the subject of hundreds of original works and many reviews (e.g., [1–12]). At the same time, the technology of synthesis of ceramics with high optical quality and reproducibility of the sample parameters has not been studied in detail so far. The problem consists, in particular, in the fact that the initial materials for synthesis of these ceramics are nanopowders with a small (about 5 nm) particle size and, therefore, with a very large surface area, the ability to absorb impurities, as well as with a strong dependence of the properties on the synthesis conditions.

There are two different approaches to obtaining oxide ceramics: non-reactive high-temperature sintering of pre-synthesised (e.g., by chemical co-precipitation) ready-to-sinter nanopowders, including a doped YAG ([2, 4–12] and references therein); and high-temperature solid-phase synthesis of nanopowders during sintering of mixtures of the initial oxides – yttrium, aluminium and activator additives ([1] and references in [3–6, 8–12]). Both approaches have their advantages and disadvantages. In chemical co-precipitation of YAG precursors, the main problem for the method of non-reactive sintering is the agglomeration of nanopowders obtained by heat treatment of the precursors [13, 14]. Figure 1 shows the YAG nanopowder produced by calcination (at 1100 °C for 2 h) of the precursor precipitated from a mixture of Y, Al and Nd nitrates. One can see numerous agglomerates – aggregation of two or more particles with the initial size of 50–80 nm into larger particles, the size of which can be up to a few microns and which may take the form of branching corals (Fig. 2).

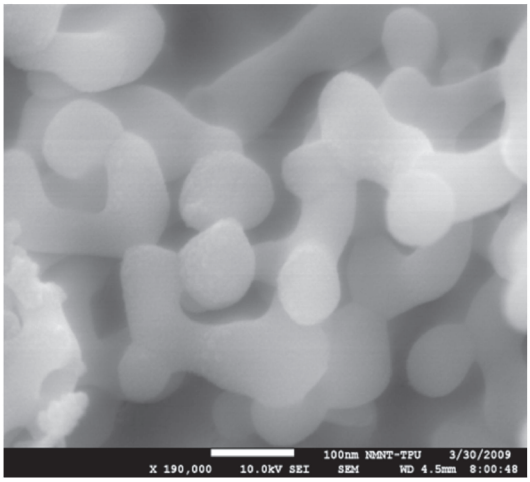

Figure 1. YAG:Nd nanopowder obtained by calcination of the precursor precipitated from nitrate solutions at 1100 °C for 2 h.

The use of chloride solutions (instead of nitrate solutions) significantly reduces the degree of agglomeration of nanopowders (Fig. 3), and the ceramics based on them have a lower (by an order of magnitude) concentration of pores, than the ceramics based YAG nanopowders synthesised from nitrate solutions. However, the results achieved are still far from optimal from the point of view of optical transmission of

S.N. Bagayev Institute of Laser Physics, Siberian Branch, Russian Academy of Sciences, prosp. Akad. Lavrent'eva 13/3, 630090 Novosibirsk, Russia; e-mail: bagayev@laser.nsc.ru;
A.A. Kaminskii A.V. Shubnikov Institute of Crystallography, Russian Academy of Sciences, Leninsky prosp. 59, 119333 Moscow, Russia; e-mail: kaminalex@mail.ru;
Yu.L. Kopylov, V.B. Kravchenko, V.V. Shemet V.A. Kotel'nikov Institute of Radio Engineering and Electronics, Fryazino Branch, Russian Academy of Sciences, pl. Akad. Vvedenskogo 1, 141120 Fryazino, Moscow region, Russia; e-mail: ylk215@ire216.msk.su, vbk219@ire216.msk.su;
A.V. Tolmachev, R.P. Yavetskiy Institute for Single Crystals, National Academy of Sciences of Ukraine, prosp. Lenina 60, 61001 Kharkov, Ukraine

Received 24 December 2012; revision received 7 February 2013
Kvantovaya Elektronika **43** (3) 271–275 (2013)
Translated by I.A. Ulitkin

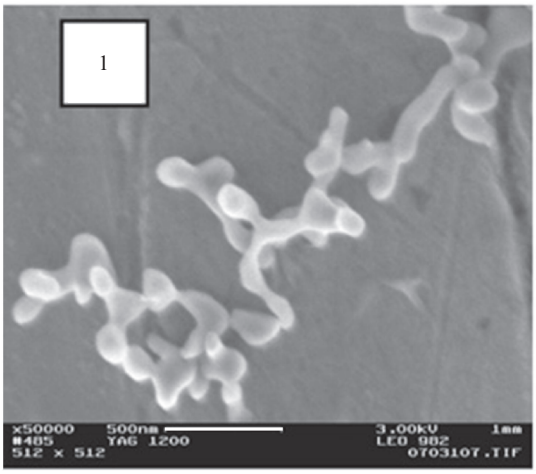

Figure 2. Coral-like YAG particle [13].

ceramics and reproducibility of their characteristics. To improve the technological process, it was decided to make use of oxide nanopowders with the lowest possible agglomeration, and best of all – with its complete absence. For oxides of rare earth elements, such powders were produced by homogeneous precipitation of oxides, which gives non-agglomerated spherical nanoparticles.

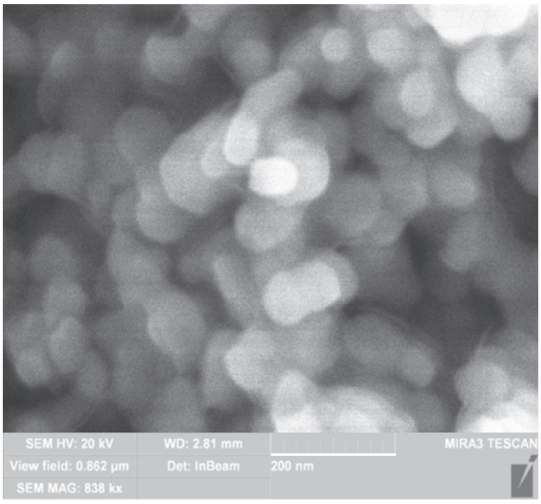

Figure 3. YAG powder produced by co-precipitation from chloride solutions at 1100 °C for 2 h.

Nanopowders of oxides of rare earth metals with spherical particle morphology are actively investigated for use in photonics, biomedicine, optics and opto-electronics, scintillation devices, etc. The spherical morphology of the initial particles and the low variance in size are favourable for a number of practical applications [13], in particular, to synthesise two-dimensional or three-dimensional fluorescent materials – display screens [15], opal-like photonic crystals [16], composite optical materials (see e.g. [17–19]) or optical nanoceramics [20, 21]. Spherical particles can be sintered to full density of 74%, close to the ideal compaction of monosized spheres [22]. As a result, compacts made of spherical particles have a low sintering temperature, which allows one to produce fine-grained ceramics with improved physical-mechanical and optical properties. Because the sintering of nanopowders depends significantly on the morphology and particle packing method, the use of spherical particles has a number of advantages compared to particles of arbitrary shape. Thus, monodisperse particles of spherical polycrystalline morphology are more active during sintering compared to single-crystal spheres of similar size [23]. Obviously, the use of spherical particles of nanometre size even allows for more dense and uniform packing of the particles in the compact compared with particles of arbitrary shape. The use of particles of different diameters makes it possible to obtain a high-density compact by filling the voids between the larger particles with a smaller fraction of the powder [24, 25].

2. Experimental technique

To obtain Y_2O_3 and $Y_2O_3:Nd^{3+}$ nanospheres (1 at. %), we used the method of homogeneous chemical co-precipitation from aqueous solutions of nitrates of yttrium and neodymium [26]. Nitrate solutions were prepared by dissolving Y_2O_3 (NO-E) and Nd_2O_3 (NO-E) during heating in an excess amount of nitric acid. The concentration of the yttrium solution was varied in the range of 0.005–0.5 mol L^{-1}. As a precipitant, use was made of the carbamide solution with a concentration of 0.3–4.0 mol L^{-1}. The mother solution was heated in a water bath to 90 °C and maintained for 2 h under constant stirring. The suspension was then cooled to 50 °C and filtered using a membrane filter. The resulting precipitate was washed at least four times with deionised water and once with ethanol, dried at 25 °C and calcined at 600–1300 °C for its transfer to the oxide phase.

Spherical nanopowders, obtained by chemical precipitation, were compacted by uniaxial dry pressing, dry pressing followed by quasi-static cold pressing, isostatic cold pressing and slip casting. These techniques are described in [14].

The compacts were sintered in a vacuum high-temperature furnace at a pressure of 3×10^{-4} Pa and a temperature of 1600 to 1750 °C. Transparent ceramic samples were obtained at a temperature close to 1650 °C. To eliminate the pores, the annealing time at the maximum temperature was 10–15 h.

3. Results and discussion

Figure 4 shows the effect of concentration of the initial reagents on the size of the spherical particles obtained by homogeneous chemical precipitation of an amorphous precursor – mixed yttrium hydroxycarbonate $Y_{1-x}Nd_x(OH)CO_3 \cdot nH_2O$. The yttrium nitrate concentration was varied in the range of 0.005–0.03 mol L^{-1} at a constant concentration of carbamide, and the concentration of carbamide – in the range of 0.3–4.0 mol L^{-1} at a constant concentration of yttrium ions. It follows from Fig. 4 that the initial concentrations of the reagents have a decisive influence on the average diameter of the precursor particles. With increasing concentration of yttrium ions in the initial solution from 0.005 to 0.02 mol L^{-1} the average particle diameter of the precursor phase increases linearly from 125 to 335 nm (Fig. 4a). At concentrations below 0.02 mol L^{-1} the precursor spheres are non-agglomerated, and the variance in the particle size does not exceed 9%. In the range of concentrations of yttrium above 0.02 mol L^{-1} the variance in the particle size increases and reaches 67% at a concentration of 0.03 mol L^{-1}. In addition, when at concentrations $C(Y^{3+}) > 0.02$ mol L^{-1}, agglomeration of the powder

particles significantly increases, individual quasi-spherical particles form agglomerates reaching the linear dimensions of a few micrometers. The dependence of the particle diameter on the concentration of carbamide $C[(NH_2)_2CO]$ is shown in Fig. 4b. The change in the concentration of carbamide from 0.3 to 2.0 mol L^{-1} is accompanied by a decrease in the average diameter of the precursor particles from 270 to 150 nm, which remains constant with a further increase in the concentration of carbamide. In the investigated range of concentrations of carbamide, the variance in the particle size $Y_{1-x}Nd_x(OH)CO_3 \cdot nH_2O$ is no more than 10%, the particles retaining their spherical shape. Thus, by varying the precipitation conditions one can control the shape, size and variance of spherical particles of the yttrium oxide precursor.

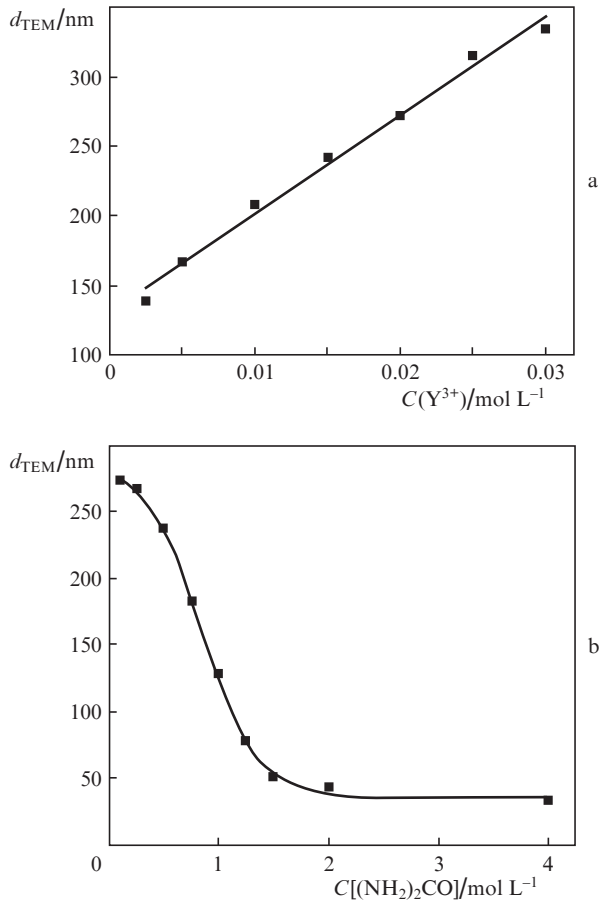

Figure 4. Average diameter of the precursor particles obtained by TEM as a function of (a) concentration of Y^{3+} ions (carbamide concentration of 0.5 mol L^{-1}) and (b) carbamide (Y^{3+} ion concentration of 0.015 mol L^{-1}).

Figure 5 shows the average diameter of the spheres and the size of individual crystallites (regions of coherent scattering) as a function of the calcination temperature. The diameter of the spheres was determined from data obtained by transmission electron microscopy (TEM), for at least 200 particles. The curve of the dependence of the average particle diameter on the calcination temperature shows two regions: up to 600 °C the particle diameter is notably reduced, and above this temperature, the diameter remains almost unchanged. Heating the precursor $Y_{1-x}Nd_x(OH)CO_3 \cdot nH_2O$ to 600 °C is accompanied by a decrease in the average particle diameter of about 23% ± 1%, which is due to the removal of reaction intermediates in the thermal decomposition of mixed basic carbonate (total weight loss of about 40%). The data of X-ray diffraction, differential thermal analysis and IR spectroscopy indicate that this temperature corresponds to the temperature of formation of yttrium oxide [26] Thus, crystallisation of $Y_2O_3:Nd^{3+}$ particles in the thermolysis of the precursor is accompanied by stabilisation of their diameter.

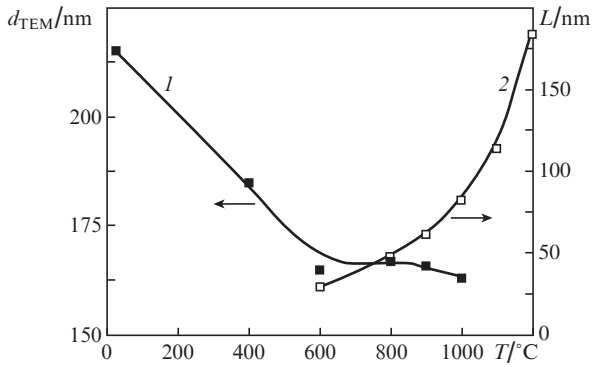

Figure 5. Diameter of (*1*) $Y_2O_3:Nd^{3+}$ (1 at. %) particles and (*2*) crystallite size vs. the calcination temperature.

As can be seen from Fig. 5, the increase in the calcination temperature of the $Y_2O_3:Nd^{3+}$ particles up to 1200 °C is accompanied by the growth of crystallite size. In the calcination temperature range 600 to 900 °C, the crystallite size varies almost linearly, whereas at higher temperatures, the slope of the curve increases significantly. These processes are related to the morphological stability of spherical particles – in the temperature range of 600–900 °C, increasing the size of the crystallites does not violate the morphology, i.e., the crystallites grow due to aggregation within the individual spherical particle. At temperatures above 900 °C re-crystallisation processes are more intense due to the interaction between neighbouring particles. As a result, the spherical particle morphology is violated.

Figure 6 shows the evolution of $Y_2O_3:Nd^{3+}$ particle morphology as a function of the calcination temperature. As shown above, crystallisation of a solid solution of $Y_2O_3:Nd^{3+}$

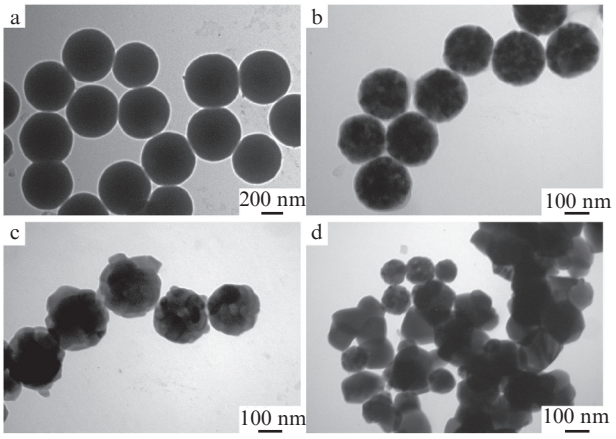

Figure 6. TEM images of (a) the precursor and $Y_2O_3:Nd^{3+}$ (1 at. %) nanospheres calcined at (b) 800 °C, (c) 1000 °C and (d) 1200 °C.

substitution is accompanied by a decrease in the average diameter of the crystallites by about 20% (Figs 6a, b). At the calcination temperature of 1000 °C, contact necks begin to form between adjacent particles (Fig. 6c), i.e., an increase in the annealing temperature increases the tendency of the particles to agglomerate. Spherical particle morphology is stable up to temperatures of 900–1000 °C, above which one can observe intense re-crystallisation and aggregation of individual particles by mass transfer through the formed contact necks into 'hard' agglomerates (Fig. 6d). The increase in the calcination temperature of spherical particles in the range from room temperature to 1200 °C is accompanied by changes in morphology and phase composition according to the following scheme: amorphous spheres $(Y_{1-x}Nd_x(OH)CO_3 \cdot nH_2O) \rightarrow$ intermediate amorphous or crystalline products $\rightarrow$ polycrystalline spheres $(Y_{1-x}Nd_x)_2O_3 \rightarrow$ aggregates of single-crystal particles $(Y_{1-x}Nd_x)_2O_3$.

Using spherical particles $(Y,Yb)_2O_3$ optical ceramics with sufficiently high transmittance were synthesised (Fig. 7). Within the standard method of compaction for the nanopowders (uniaxial pressing, then quasi-isostatic pressing at a pressure of 250 MPa) the best transmission (over 83% in the region of 1 μm) was obtained by the addition of approximately 10% conventional, finely ground powder reagent La_2O_3 to spherical nanoparticles $(Y,Yb)_2O_3$. Ceramics made of nanospheres $(Y,La,Yb)_2O_3$ had somewhat smaller transmission, which testified to the need for selection a modified method of compaction in this case.

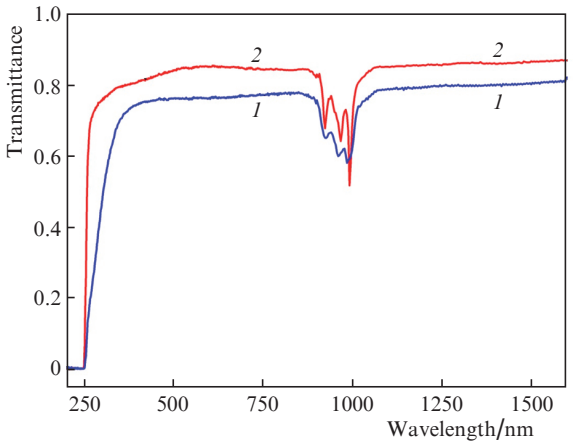

Figure 7. Optical transmission of $(Y,La,Yb)_2O_3$ ceramics prepared using only (*1*) $(Y,La,Yb)_2O_3$ nanospheres and (*2*) a mixture of $(Y,Yb)_2O_3$ nanospheres and finely-ground La_2O_3 powder.

Samples of Y_2O_3:Nd nanopowders with a spherical shape of the particles, containing up to 4 at. % neodymium, were used to obtain YAG:Nd ceramics. As a source of aluminium oxide (after testing a number of commercial aluminium oxide nanopowders), use was made of Al_2O_3 (Baikovski, France). Figure 8 shows a photograph of the powder sample. One can see that the agglomeration of the particles in it is virtually very small, and the average particle size is about 100–150 nm. Figure 9 presents a photograph of ceramic neodymium-doped YAG samples synthesised using these nanopowders. Staining some YAG samples with red colour is due to the presence of technological impurities of zirconium oxide and the formation of three-valent zirconium during sintering. This colour disappears after annealing in air.

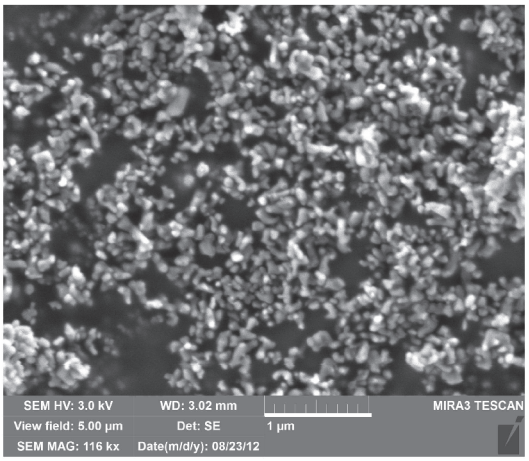

Figure 8. Al_2O_3 powder (Baikovski, France).

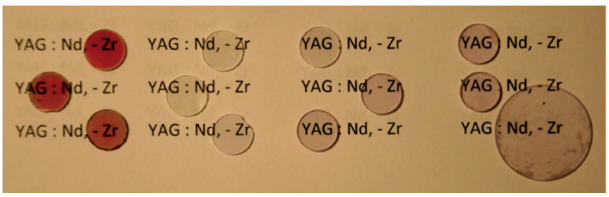

Figure 9. Appearance of YAG:Nd ceramic samples. Diameter of small samples is 10 mm.

Figure 10 shows the spectrum of the optical transmission of one of the ceramic YAG:Nd samples after annealing in air. The transmittance at a sample thickness of 1 mm in almost all samples was at least 81%, and in a number of samples the transmittance exceeded 83% near 1 μm, indicating good reproducibility of technology. A sharp rise in the transmittance in the short-wavelength spectrum testifies to a low concentration of the pores. Under the microscope the pore concentration was found to be a few ppm.

Thus, the method of synthesis of initial non-agglomerated yttrium oxide nanopowders provides obtaining samples of high optical quality Y_2O_3 and YAG laser ceramics. Of course,

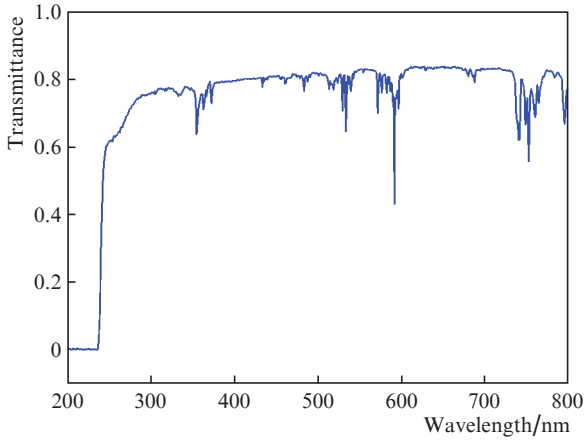

Figure 10. Spectrum of optical transmission of YAG:Nd ceramic samples. The sintering temperature is 1615 °C, the average grain size is 2 μm.

the method can be used for other rare earth oxides. Thus, spherical particles with an average diameter of 50–350 nm and a variance in size no greater than 10% can be obtained by homogeneous co-precipitation for a $(Lu_{1-x}Eu_x)_2O_3$ system, which is quite promising for synthesis of transparent phosphors due its composition [27, 28].

4. Conclusions

We have considered the problems of agglomeration of yttrium aluminium garnet nanopowders prepared by chemical co-precipitation of precursors from aqueous solutions and subsequent calcination. Agglomeration leads to the pores in the samples of YAG laser ceramics, increased transmission losses and poor reproducibility of the characteristics of the samples. To obtain samples of YAG laser ceramics and yttrium oxide with high transparency and good reproducibility of the characteristics, we have developed a method of synthesising non-agglomerated nanopowders of pure and doped yttrium oxides by homogeneous chemical precipitation. The nanopowders obtained have virtually perfect spherical shape, and the particle size can be controlled by the experimental conditions. After compacting nanopowders Y_2O_3 with La and Yb as well as mixtures of Y_2O_3:Nd and several commercial nanopowders of aluminium oxide, we have selected the best nanopowders and methods of compaction. Besides, using solid-phase synthesis in a vacuum sintering we have obtained ceramic samples of $(Y, La, Yb)_2O_3$ and neodymium-doped YAG with high optical transmittance near 1 μm.

Acknowledgements. The authors of Institute for Single Crystals, National Academy of Sciences of Ukraine (A.V.T. and R.P.Ya.) thank Yu.I. Pazura for his help in preparing the experimental samples. This work was partially supported by the programme 'Extreme Light Fields and Their Applications' of the Presidium of RAS, the Russian Foundation for Basic Research (Grant Nos 11-02-90465-Ukr_f_a, 10-02-00705-a and 11-02-ofi-m-2011) and the State Fund for Fundamental Research (Project F40.7/061).

References

1. Ikesue A., Kinoshita T., Kamata K., Yoshida K. *J. Am. Ceram. Soc*., **78**, 1033 (1995).
2. Lu J., Lu J., Murai T., et al. *OSA Tops. Adv. Sol.-State Lasers*, **68**, 507 (2002).
3. Ikesue A., Aung Y.L., Taira T., et al. *Annu. Rev. Mater. Res*., **36**, 397 (2006).
4. Kaminskii A.A. *Laser & Photon. Rev*., **1**, 93 (2007).
5. Ikesue A., Aung Y.L. *Nature Photon*., **2**, 721 (2008).
6. Taira T.C.R. *Physics*, **8** (2), 138 (2007).
7. Garanin S.G., Dmitriuk A.V., Zhilin A.A., et al. *J. Opt. Techn*., **77**, 52 (2010).
8. Sanghera J., Kim W., Villalobos G., et al. *Proc. SPIE Int. Soc. Opt. Eng*., **8039**, 803903-1-8 (2011).
9. Sanghera J., Bayya Sh., Villalobos G., et al. *Opt. Mater*., **33**, 511 (2011).
10. Garanin S.G., Dmitriuk A.V., Zhilin A.A., et al. *J. Opt. Techn*., **78**, 60 (2011).
11. Taira T. *Opt. Mater. Express*, **1**, 1040 (2011).
12. Boulon G. *Opt. Mater*., **34**, 499 (2012).
13. Kopylov Yu.L., Kravchenko V.B., Bagayev S.N., et al. *Opt. Mater*., **31**, 707 (2009).
14. Bagayev S.N., Kaminskii A.A., Kopylov Yu.L., Kravchenko V.B. *Opt. Mater*., **33**, 702 (2011).
15. Cho S.H., Kwon S.H., Yoo J.S., et al. *J. Electrochem. Soc*., **147**, 3143 (2000).
16. Lin S.-E., Yu B.-Y., Shuye J.-J., Wei W.-C.J. *J. Amer. Ceram. Soc*., **91**, 3976 (2008).
17. Pritula I., Bezkrovnaya O., Kolybayeva M. *Mater. Chem. Physics*, **129**, 777 (2011).
18. Pritula I.M., Kosinova A.V., Vorontsov D.A., et al. *J. Crystal Growth*, **355**, 26 (2012).
19. Grachev V.G., Vrable I.A., Malovichko G.I., et al. *J. Appl. Phys*., **112**, 014315 (2012).
20. Fukabori A., Yanagida T., Pejchal J., et al. *J. Appl. Phys*., **107**, 073501 (2010).
21. Podowitz S.R., Gaume R., Feigelson R.S. *J. Amer. Ceram. Soc*., **93**, 82 (2010).
22. Rhodes W.H. *J. Amer. Ceram. Soc*., **64**, 19 (1981).
23. Slarnovich E.B., Lange F.F. *J. Amer. Ceram. Soc*., **73**, 3368 (1990).
24. Coble R.L. *J. Amer. Ceram. Soc*., **56**, 461 (1973).
25. Lange F.F. *J. Amer. Ceram. Soc*., **72**, 3 (1989).
26. Pazura Yu.I., Baumer V.N., Deyneka T.G., et al. *Funct. Mater.*, **17**, 107 (2010).
27. Babayevskaya N.V., Deyneka T.G., Mateychenko P.V., et al. *J. Alloys and Compounds*, **507**, L26 (2010).
28. Dulina N.A., Deineka T.G., Yavetskiy R.P., et al. *Ceram. Intern*., **37**, 1645 (2011).